

# Influence of endodontic chemical treatment on *Enterococcus faecalis* adherence to collagen studied with laser scanning confocal microscopy and optical tweezers: a preliminary study

## CheePeng Sum

National University of Singapore  
Department of Restorative Dentistry  
Faculty of Dentistry  
5 Lower Kent Ridge Rd.  
Singapore 119074

## Samarendra Mohanty\*

### P. K. Gupta

Raja Ramanna Centre for Advanced Technology  
Biomedical Applications and Instrumentations Division  
Indore 452013, India

## Anil Kishen

National University of Singapore  
Department of Restorative Dentistry  
Faculty of Dentistry  
5 Lower Kent Ridge Rd.  
Singapore 119074

**Abstract.** Failure of endodontic treatment is commonly associated with the presence of *Enterococcus faecalis*. Studies have highlighted that *E. faecalis* can form a calcified biofilm in tough environmental conditions, such as within root canals. The aims of this study were to investigate the effects of chemicals used in root-canal disinfection on the adherence of *E. faecalis* to collagen, as well as to estimate the force of adhesion between *E. faecalis* and collagen after such treatment. The number of adhering bacteria after chemical treatment was determined using confocal laser scanning microscopy-based adherence assay. It was found that the calcium hydroxide-treated group had a statistically significant ( $p=0.05$ ) increase in the population of bacteria adhering. The adhesion force between bacteria and collagen of the treatment group with the highest number of bacteria adhering was determined by using optical tweezers (1064 nm) and Equipartition theorem-based stiffness measurements. The presence of calcium hydroxide was found to significantly increase the bacterium-collagen adhesion force. These experiments highlighted the potential advantage of using optical tweezers to study bacteria-substrate interactions. The findings from the present study suggests that the presence of calcium hydroxide increased the adhesion force and adherence of *E. faecalis* to type-I collagen. © 2008 Society of Photo-Optical Instrumentation Engineers. [DOI: 10.1117/1.2957972]

Keywords: type-I collagen; *Enterococcus faecalis*; bacteria adhesion; endodontic treatment; confocal microscopy; laser tweezers.

Paper 07257RRR received Jul. 13, 2007; revised manuscript received Mar. 11, 2008; accepted for publication Mar. 12, 2008; published online Jul. 24, 2008.

## 1 Introduction

The organic phase of dentine, among other proteins, consists of both type-I and -III collagen. However, type-I collagen forms the bulk of the matrix of dentine.<sup>1</sup> The inorganic phase of dentine is composed of a carbonate-rich but calcium-deficient hydroxyapatite and forms ~50 vol % of the substance of dentine.<sup>2</sup> In many types of dental treatment where dentine is exposed to chemicals, removal of the inorganic calcified phase by chemicals such as ethylenediamine tetra-acetic acid (EDTA), exposes the organic phase (mostly type-I collagen). The propensity for bacteria to adhere to surfaces may determine the likelihood of biofilm-mediated infection, because adhesion is the first step to colonization and biofilm formation. Much effort has gone into attempts to reduce bacterial adhesion to medical devices so as to reduce the rates of biofilm-mediated infections.<sup>3</sup> Biofilms have been found in the

apical portion of the root canals of teeth with periapical pathology.<sup>4</sup> Studies have shown that *Enterococcus faecalis* in biofilm can survive starvation for extended durations.<sup>5</sup> It has also been shown that *E. faecalis* adhere to dentine in the presence of serum and collagen.<sup>6</sup> Several other studies have also shown that *E. faecalis* is the most prevalent microorganism associated with root canals with posttreatment periapical lesions.<sup>7-9</sup>

The atomic force microscope has become an accepted tool to measure interaction forces between bacteria and substrates.<sup>10,11</sup> However, use of positively charged polymers, such as poly-ethyleneimine and poly-L-lysine, is necessary to securely attach bacteria onto the cantilever tips. In addition, glutaraldehyde is often used to treat the bacteria as a cross-linker.<sup>12</sup> The physical attachment of bacterial cells using positively charged polymers may promote structural rearrangements in bacterial cell surface structures,<sup>13</sup> while glutaraldehyde treatment has been shown to induce physicochemical as well as mechanical alterations to bacterial cell surfaces.<sup>14</sup> These chemical treatments can alter the forces

\*Presently at Beckman Laser Institute, 1002 Health Science Road East, University of California—Irvine, Irvine, CA 92612.  
Address all correspondence to: Anil Kishen, Restorative Dentistry, National University of Singapore, National University Hospital—5 Lower Kent Ridge Road, Singapore 119074.

**Table 1** Treatment groups of collagen membranes.

Group 1	Saturated solution of calcium hydroxide (24 h)
Group 2	Chlorhexidine 0.2% (1 h)
Group 3	0.05% NaOCl (1 h).
Group 4	Control

measured and compromise the results. In contrast, laser tweezers<sup>15</sup> is a noninvasive and noncontact tool that can probe interaction between microscopic objects (such as bacteria and collagen) with sub-pN sensitivity.

Understanding the effect of different chemicals, used clinically during root-canal treatment (RCT), on the adherence of *E. faecalis* to type-I collagen, would contribute to the further understanding of how this bacterium forms biofilm on dentine substrate and survive the tough environmental conditions prevailing in a root-canal treated tooth. Chemicals, however, have many effects on collagen, and the increase in bacterial adherence may just be mere physical retention of bacteria on the substrate. Further collagen membranes are meshlike networks of collagen fibrils, and alterations in the number of bacteria adhering on a treated membrane may be linked to the variations in the mesh densities of membranes after chemical treatment and may not be due to an increase in adhesion force. Therefore, it is imperative to measure the adhesion force between bacteria and substrate after a chemical treatment to be able to attribute the increase in adherence directly to an increase to adhesion force. The aims of our experiments are (1) to examine *E. faecalis* adherence to type-I collagen after treatment with chemicals commonly employed in RCT using confocal laser scanning microscopy (CLSM)-based bacterial adherence assay and (2) to measure the force of adhesion, between *E. faecalis* and type-I collagen, in the group with the highest number of bacteria adhering using laser tweezers-based trap stiffness measurement.

## 2 Experiments

### 2.1 Sample Preparation

The eggshell membrane type-I collagen model was used in this study. Eggshells obtained were cleaned with detergent, and the eggshell membrane was carefully removed. The cleaned eggshell was placed in 1 M hydrochloric acid. After 1 h, the decalcified collagen membrane is carefully removed and washed in distilled water. The membrane was then soaked overnight in an acid solution of bovine pepsin (Roche, Switzerland) to remove all noncollagenous proteins.<sup>16</sup> The collagen membrane was carefully cut to size, about 10 × 8 mm using sterile surgical scissors, and then placed under ultraviolet (UV) light for 1 h to kill any bacteria. The prepared membrane pieces were then treated by various chemicals commonly used in RCT as shown in Table 1. The membranes were soaked in saturated calcium hydroxide solution (Fluka, Switzerland) for 24 h, in chlorhexidine (10% diluted Hibis-

crub, Regent Medical, UK) for 1 h and 0.05% sodium hypochlorite (Chlorox, USA) for 1 h.

The prepared membranes were then thoroughly rinsed in distilled water for 1 min and put into an overnight culture of *E. faecalis* ATCC 29212 in All Culture (AC) broth (Sigma Aldrich, USA), with number of *E. faecalis* cells adjusted to an optical density equivalent to 10<sup>8</sup> cells/ml. After 1 h, the membranes were removed and vortexed at 3000 rpm (Barnstead Maxi Mix II, Type 37600, USA) in a 20 ml falcon tube containing 10 ml of PBS for 1 min to remove any loosely adherent cells. The maximum relative centrifugal force exerted by the vortex mixer was calculated to be 450 G. The membranes were carefully spread onto a microscope slide and stained with LIVE/DEAD BacLight bacterial viability stain (Molecular Probes, USA), following manufacturer's instructions and then covered with a coverslip for further examination in a CLSM.

### 2.2 CLSM-Based Bacterial Adherence Assay

The specimens were examined in a CLSM (Olympus FV 500, Japan) set to monitor fluorescein isothiocyanate and propidium iodide. Confocal illumination was provided by a Kr/Ar laser excitation (488 nm) fitted with a long-pass 514 nm emission filter. A 580 nm beamsplitter was used together with a long-pass 520 nm filter (green fluorescent signal) and a long-pass 590 nm filter (red fluorescent signal). Simultaneous dual-channel imaging using pseudocolor was used to display green and red fluorescence. Specimens were imaged using 60X oil immersion objective (Olympus, Japan). When a field was viewed, it was digitally captured, after optimizing the image into a computer, and the image stored. Then, the XY table, which is equipped with a micrometer, was turned at least two and a half turns. This moves the stage by ~250 μm in each of the X and Y axes, clearly onto a new field of view. A total of nine fields were examined for each treatment, and the bacteria present were counted. The nine fields were made up of three fields each from three similarly treated samples, inoculated by bacteria from the same culture. Only bacteria in focus of each optical section were counted. The counting was carefully done by one operator using a manual digital counter so that the same bacterium was not counted twice. The different treatment groups of collagen membranes, studied using CLSM, are listed in Table 1.

### 2.3 Laser Tweezers Experimental Setup

A schematic of the laser micromanipulation setup is shown in Fig. 1. The output of a 1064 nm CW Nd:YAG laser (SSLD, CAT, India) operating in fundamental Gaussian mode was expanded using a beam expander (BE) and coupled to the objective of an inverted microscope (Axiovert 135TV, Carl Zeiss) through its base port via a folding mirror (M2) that retains its regular fluorescence imaging configuration and capability. Another convex lens (SL,  $f=200$  mm) was placed into the optical path of the beam external to the microscope. This lens along with the tube lens of the microscope behaves as a 1:1 telescope, and thus, a collimated beam is sent to the 100X microscope objective. A 100X Plan Neofluor oil immersion phase objective was used to focus the laser beam to a diffraction-limited spot. The dichroic mirror reflects the UV-visible light from the excitation source (mercury lamp, HBO)

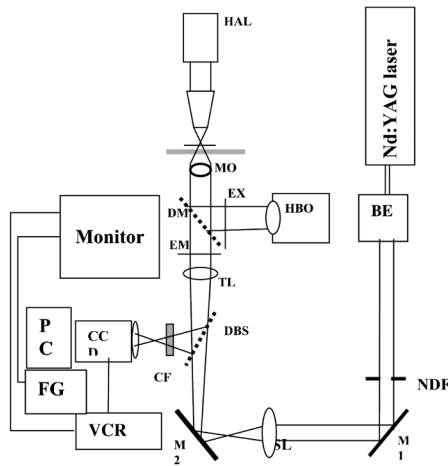


**Fig. 1** Schematic of the experimental setup. BE: beam expander; NDF: neutral density filter; MO: 100× Plan Neofluor phase objective; SL: spherical lens; TL: tube lens; HAL: halogen lamp; DBS: dichroic beam splitter; HBO: mercury lamp; DM: dichroic mirror; EX: excitation filter; EM: emission filter; CF: IR cutoff filter; and FG: frame grabber.

through the excitation filter and transmits the fluorescence. The dichroic beamsplitter transmits the cw 1064 nm and reflects the emitted fluorescence through the emission filter to the CCD. An infrared cutoff filter was placed before the CCD to reject the backscattered laser light. The fluorescence images were captured using a cooled CCD and processed using Q-Fluoro standard image analysis software (Leica). The bright-field trapping sequences were recorded using video CCD onto a VCR, and digitized using a frame grabber.

The CW Nd:YAG laser-trapping beam power was adjusted to attain powers up to 200 mW at the focal plane of the objective. The trapping laser beam power at the back aperture of the objective was monitored with a power meter (Scientech, USA). Furthermore, for estimating the transmission factor of the objective, the dual-objective method was adapted in order to correct for the total internal reflection losses at the objective-oil-glass-water interfaces. The transmission factor of two cascaded objectives was found to be 0.33. From this, the transmission factor of a single 100 X Plan Neofluor phase objective (Carl Zeiss, Germany) was estimated to be  $(0.33)^{1/2}$  (i.e., 0.57).

To determine the position of a bacterium in a video frame, the method of centroid detection was used. Software program on LabView platform (National Instruments, USA) was developed for quick analysis of a large number of images. The region of interest selection and thresholding was carried out in order to reject background images of other objects (such as collagen fiber) outside the trap. For determination of tracking resolution, a bacterium was fixed on the coverslip and the position of its center was measured using the software for ~1000 time-lapse (40 ms) digitized frames. For *E. faecalis* bacterium, a tracking resolution of better than 50 nm (standard deviation of position histogram) was obtained. For force measurements using optical tweezers, eggshell membranes were obtained as described in Section 2.1. *E. faecalis* was grown overnight and diluted using AC broth to  $\sim 10^4$  cells per milliliter. The prepared collagen membrane, whether treated

by calcium hydroxide or not, was carefully spread onto a clean glass slide and the edges teased under magnification to obtain frayed edges with single strands of collagen fibers. A small volume of AC broth with the adjusted bacteria concentration,  $\sim 200 \mu\text{l}$ , was applied onto the membrane and a cover clip was placed over it and the entire system was sealed. A single bacterium was trapped and moved in order to measure the trapping force and stiffness. Then the bacterium was brought to the single collagen fibers with the optical tweezers and manipulated to check to see if it was in plane with the fiber. The bacterium was then held in place for varying durations, and then, its mean position was measured in order to estimate the interaction force. At the end of  $\sim 10$  min, the rupture force was measured by pulling the trapped bacterium away from the fiber using the optical tweezers of varying laser power. For this experiment, type-I collagen membrane was soaked for 5 min in a media that contained 50% AC broth and 50% saturated  $\text{Ca}(\text{OH})_2$ . The membrane was spread onto a glass slide, onto which diluted bacterial suspension was added. The force of laser tweezers on the bacteria was estimated at different trap power levels using the escape force method, and trapping stiffness was calculated using the Equipartition theorem method. Different treatment groups of collagen membranes, studied using optical tweezers, are listed in Table 2.

### 2.3.1 Force calibration using escape force method

In this method of force calibration,<sup>15,17</sup> a single bacterium was trapped at different power levels and translated. The velocity was progressively increased until it escaped from the optical trap. The limiting velocity was derived using the method described above, and the corresponding viscous drag force was calculated. The *E. faecalis* bacterium was assumed to be spherical in shape with a diameter of  $\sim 0.5 \mu\text{m}$ .<sup>18</sup> When the bacterium is more than a few diameters away from the sample cell walls, the viscous drag exerted by moving the stage or the bacterium (of diameter  $d$ ) at a velocity  $v$  and is given by Stoke's law

$$F = 3\pi\eta dv. \quad (1)$$

Here,  $\eta$  is the viscosity of the medium ( $0.001 \text{ Kg m}^{-1} \text{ s}^{-1}$ ). For a specified laser power, the critical velocity at which the trapped bacterium comes out of the trap determines the trapping force. For a trapping power of 50 mW, the limiting velocity was found to be  $90 \mu\text{m/s}$  and this corresponds to a viscous drag force of 0.52 pN. Repeating this experiment for other laser powers gives a “force versus laser power” calibration curve and it scales linearly (Fig. 2) with the laser power for a particular size and refractive index of the object (bacterium). The slope of the linear fit (Fig. 2) provides an estimate of the trapping efficiency for *E. faecalis* bacterium.

The trapping efficiency of the optical tweezers is described in terms of a dimensionless parameter  $Q$ , the fraction of momentum transferred to the trapping force from the trapping laser beam, which is related to the force on the bacterium  $F$ , the power of the laser  $P$ , and the refractive index of the surrounding medium ( $n=1.33$ ), through

**Table 2** Treatment groups of collagen membranes for studying adhesion using optical tweezers.

No. of Bacteria	Treatment Groups	Result
3	Collagen soaked with 75% calcium for 15 min	No attachment up to 20 min
4	Collagen soaked with 50% calcium for 15 min	Firmly attached in 6.5 min
4	Collagen soaked with 50% calcium+ 50% AC media for 5 min	Two are firmly attached in 5 min and other two could be pulled apart by optical tweezers
5	Collagen not soaked with calcium	No attachment up to 15 min
3	Collagen overnight with 50% Calcium and 50% AC media	Attached in 10 min, but could be detached at laser power of 180 mW
4	Collagen overnight with 25% Calcium and 75% AC media	No attachment upto 5 min

$$F = nQP/c. \quad (2)$$

Using the slope of the linear fit [ $\sim 0.0123$  (Fig. 2)], the lateral trapping efficiency of optical tweezers  $Q$  (lateral) for the *E. faecalis* bacterium was found to be as low as  $\sim 0.3\%$ . For dielectric particles, the trapping force (hence, efficiency) has been seen to decrease as linearly with  $r$  as particle size increases beyond the focused spot size ( $\sim 0.8 \mu\text{m}$ ). For Rayleigh (size of particle  $\ll \lambda$ ) particles, trapping efficiency decreases more rapidly ( $\sim r^3$ ) because the gradient force is proportional to polarizability ( $\alpha$ ), which depends on the particle radius ( $r$ ) as  $r^3$ . In addition to very small radius of the *E. faecalis* bacterium ( $\sim 0.25 \mu\text{m}$ ), because the relative refractive index of the bacterium with respect to the surrounding medium is also quite small, the theoretical values for  $Q$  is expected to be very small. Because of this small value of trapping efficiency, the maximum trapping force that can be

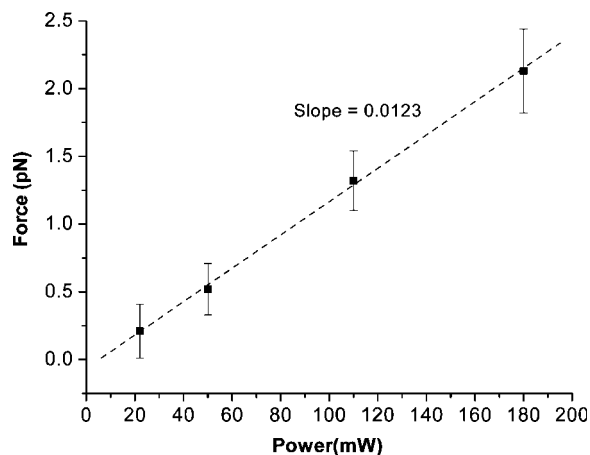


**Fig. 2** Power versus trapping force on *E. faecalis* bacterium. The error bars represent standard deviation from measurements on four *E. faecalis* bacteria.

applied to the *E. faecalis* bacterium was limited to  $\sim 2$  pN at the maximum trapping power of 180 mW. Application of larger trapping power was limited, because it can lead to loss of viability of the bacterium.

### 2.3.2 Measurement of trap stiffness using equipartition theorem method

Forces acting in a trap are described by Hooke's law:  $F = -K_{\text{trap}}X$ . Using the trap to determine the force exerted by a bacterium therefore required calibration of its stiffness  $K_{\text{trap}}$ . The trap stiffness was determined by use of the equipartition theorem,

$$\frac{1}{2}K_{\text{trap}}\langle x^2 \rangle = \frac{1}{2}K_{\text{B}}T, \quad (3)$$

where  $K_{\text{B}}$  is the Boltzmann constant and  $T$  is the temperature of the medium in which the bacterium was suspended. Measuring the variance of the position of the trapped bacterium provides an estimate of trap stiffness,

$$K_{\text{trap}} = K_{\text{B}}T/\text{Var}\langle x \rangle. \quad (4)$$

The chief advantage of this method is that knowledge of the viscous drag coefficient is not required and, therefore, of the bacterium shape as well as fluid viscosity. The transverse positions of a bacterium in the trap are detected using the centroid detection method, and a representative track over 50 frames (i.e., for 2 s) is shown in Fig. 3(b). The bacterium can be seen to be around one most probable position, which is the center of the trap focus (here, pixel number 11). Frequency count at different positions of the bacterium inside the trap is done, and the variance of the position of the trapped bacterium is calculated. The stiffness of the optical trap was then calculated using Eq. (4), and this experiment was repeated at different trapping power levels. The stiffness versus laser power graph was plotted [Fig. 3(c)].

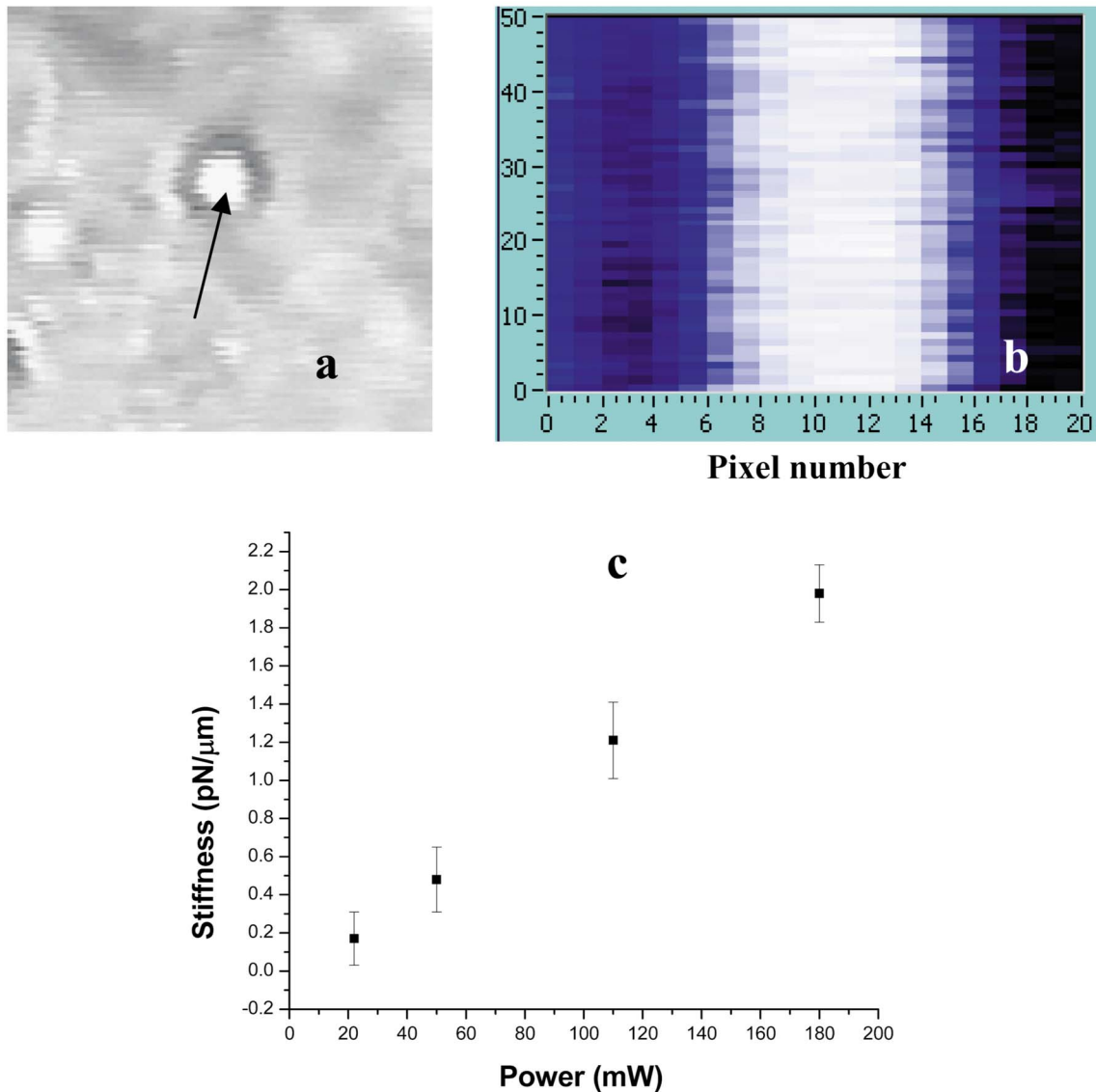


**Fig. 3** (a) Trapping of *E. faecalis* bacterium (arrow marked) and (b) timetrack of the trapped bacterium over 50 frames. The x axis in (b) is in units of CCD pixels and y axis is the frame number. The timetrack in (b) is generated by integrating the intensities in one direction (say Y) in each image frame and displaying it as one line for each frame. (c) Trapping stiffness is shown as a function of laser power for *E. faecalis* bacterium. The error bars represent standard deviation from measurements on four *E. faecalis* bacteria.

### 3 Results

#### 3.1 CLSM-Based Bacterial Adherence Assay

The histogram depicting the bacterial count for different treatment groups is shown in Fig. 4(e). Using one way ANOVA with multiple comparisons, significantly more bacteria were found adhering to the samples treated with calcium hydroxide [Ca(OH)<sub>2</sub> group] than control, as well as those treated by NaOCl and chlorhexidine ( $P=0.05$ ). The chlorhexidine-treated group had the least bacteria adhering and had significantly less bacteria than all the other groups. There was no significant difference between the NaOCl-treated group and control. CLSM images of collagen membranes treated with the different chemicals and inoculated with bacteria are shown in Fig. 4(a)–4(d).

#### 3.2 Optical Tweezers–Based Study on Interaction Between Bacteria and Collagen

Figure 5 shows digitized images of bacteria on the collagen matrix. Large numbers of adhering bacteria were found [Fig. 5(b)] on collagen membranes treated with calcium as compared to those collagen without calcium treatment [Fig. 5(a)]. In order to assess the adhesion of bacteria with collagen under various treatment conditions, use of optical tweezers was employed. During experiments with the use of the optical tweezers, a single bacterium was brought near a collagen fibril and the time taken by the bacterium to attach with the collagen fibril was measured. Studies on the different treatment groups listed in Table 2 (based on a varying fraction of calcium, duration of soaking, etc.) showed that maximum bacterial ad-

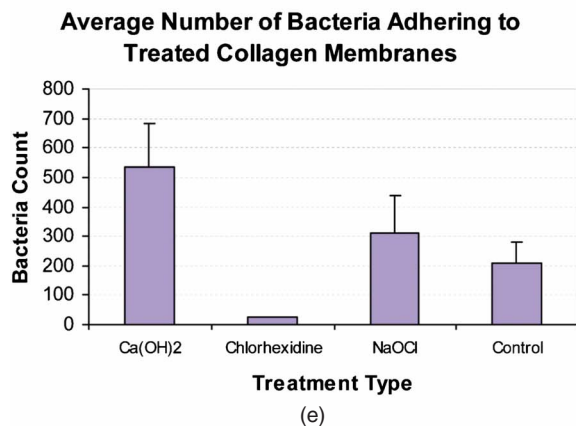
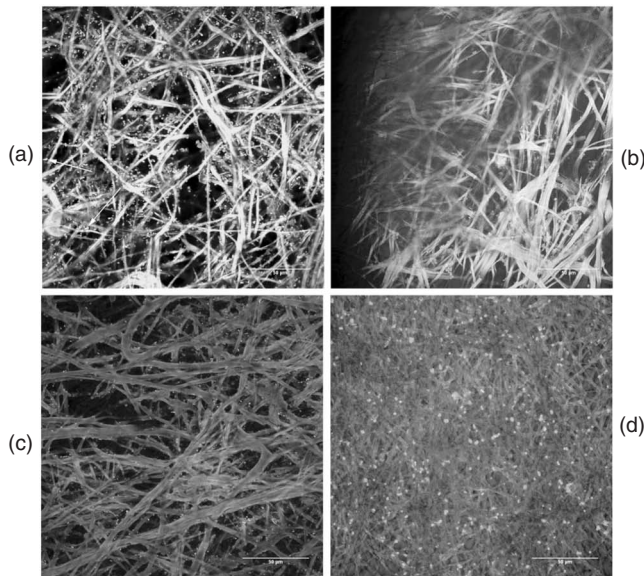


**Fig. 4** Collagen treated with various chemicals: (a) Calcium hydroxide (arrows pointing to plaque-like masses), (b) chlorhexidine, (c) control, (d) NaOCl, (e) graph showing average number of bacteria adhering.

hesion occurs for collagen soaked with 50% calcium hydroxide as compared to 0% or 25% or 75% calcium hydroxide.

### 3.2.1 Force measurement using laser tweezers

Because the collagen was soaked with 50% calcium for 15 min, the bacteria was found to firmly attached in ~6.5 min, detachment of the bacterium could not be accom-

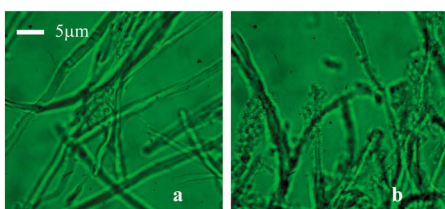


**Fig. 5** Overnight culture of bacteria on collagen fibre matrix: (a) without calcium treatment and (b) with overnight calcium treatment.

plished at the highest laser power used (180 mW). Therefore, instead of rupture force measurement, continuous measurement on the interaction of bacteria was made using laser tweezers. Figure 6 shows the time track of interaction of *E. faecalis* bacterium with collagen. After a duration of interaction, the mean position [black lines in Fig. 6(b)] of bacterium was found to shift toward the collagen fibril. A cartoon depicting interaction force measurement using the displacement ( $\Delta x$ ) of the bacterium from its mean position in the presence of collagen is shown in Fig. 7. From the predetermined stiffness of trap ( $K_{\text{trap}}$ ) for *E. faecalis* bacterium in the absence of collagen (see Fig. 3), the interaction force was determined using

$$F = K_{\text{trap}} \Delta x. \quad (5)$$

For a fixed interaction period of 5 min, the interaction force was found to increase from 0.03 pN when the collagen is not treated with calcium to 0.9 pN in case of calcium treated collagen fibers. Furthermore, in calcium-treated collagen, the interaction force increased with increase in the time of interaction of bacterium with collagen (Table 3). In some cases, at small interaction durations, the bacterium could be detached from the collagen fibril by increasing the laser power to 180 mW and, thus, rupture force could be measured for short interaction durations (~5 min). These results are listed in Table 3. The mean rupture force was significantly lower (0.38 pN, corresponding to a trap beam power of 36 mW, obtained from Fig. 2) in absence of calcium as compared to the case of the calcium-treated ones (2.1 pN, at 180 mW, see Fig. 2).

## 4 Discussion

Recently, MTAD, an acidic proprietary irrigant (pH 2.2), has shown promising results as an antimicrobial cleaning agent to remove smear layer as the final rinse.<sup>19</sup> Though it had not been reported that this acidic solution would remove the calcified phase of dentine to expose collagen, it is reasonable to believe that any acid would likely decalcify dentine and lead to collagen exposure. It had been reported that up to 3.8% by volume of a liquid irrigant, EDTA, remained in the root canal after irrigation.<sup>20</sup> It is reasonable and logical to believe that a similar volume of MTAD may not be completely removed from the tooth when it is used as an irrigant; the acidic remnants would continue to remove calcium until the chemical is spent. Hence, any practitioner who uses either of these chemicals as the last irrigants would likely expose collagen. Exposed collagen is a substrate for many species of oral bacteria, including *E. faecalis*.<sup>21</sup> After RCT, bacteria may be left behind in the dentinal tubules (residual bacteria).<sup>22</sup> These can reseed the chemically treated root-canal dentine and make use of the collagen to adhere and survive the tough environmental conditions prevailing in an endodontically treated tooth.

In addition to residual bacteria, microleakage (fluid leakage between dentine and the restoration) can also allow bacterial reentry into the root-canal space. Because dentine collagen is largely type-I collagen and our hypothesis was that chemical alteration of collagen by endodontic irrigating solutions and medicaments causes an increase in bacterial adhesion, in this study we used a model of type-I collagen membrane to study their effects on collagen.

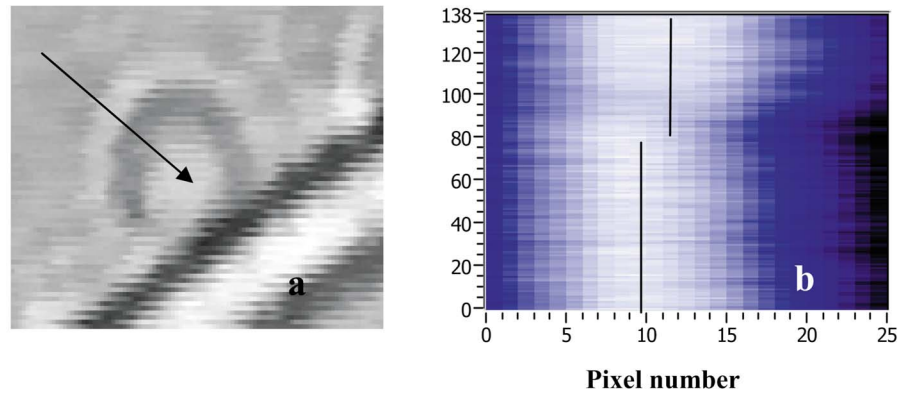


**Fig. 6** Interaction of *E. faecalis* bacterium with collagen: (a) A trapped *E. faecalis* bacterium was brought in the vicinity of a collagen fiber from a direction indicated by arrow, (b) timetrack of the trapped bacterium over 138 frames. The x axis in (b) is in units of CCD pixels and the y axis is the frame number. The timetrack in (b) is generated by integrating the intensities in one direction (say Y) in each image frame and displaying it as one line for each frame. The change in mean position [black lines in (b)] toward collagen present in the right-hand side can be noted.

Eggshell membrane normally is coated with a layer of type-X collagen on type-I collagen, which forms the bulk of the membrane. After treating the eggshell membrane in pepsin overnight, the type-X collagen was removed and only type-I collagen remained.<sup>23</sup> We therefore used this as a model to study bacterial interaction with chemically treated type-I collagen. CLSM showed that bacteria adhered to all samples of type-I collagen membrane treated by chemicals commonly used in RCT. Very few bacteria were detected on specimens treated with chlorhexidine. We observed that in those mem-

branes treated by calcium hydroxide (group 1), there were more thick plaque-like masses [arrowed in Fig. 4(a)] aggregating on the surfaces of the collagen fibrils. These plaques were bigger than individual *E. faecalis* cells. However, it was not possible for us to clearly say that these plaques comprised only bacteria, though it seems clear that they are of bacterial origin. It was also not possible for us to clearly count the number of bacteria cells in each of these aggregates. Some species of bacteria have been observed to secrete extracellular polymeric substances (EPS), which aid in biofilm formation.<sup>24</sup> We do not know that *E. faecalis* produces EPS, but we do know that it forms biofilms.<sup>25</sup> Note that the irrigants we used in these experiments were 0.2% chlorhexidine and 0.05% NaOCl and saturated calcium hydroxide solution, instead of the commonly used concentration of 2% and 5.25% and a paste, respectively, in the clinical setting. This was because the membrane is a thin mesh of collagen fibrils and is easily penetrated by these chemicals, and using a strong concentration of NaOCl (5.25%) would completely dissolve the membrane in a short time.

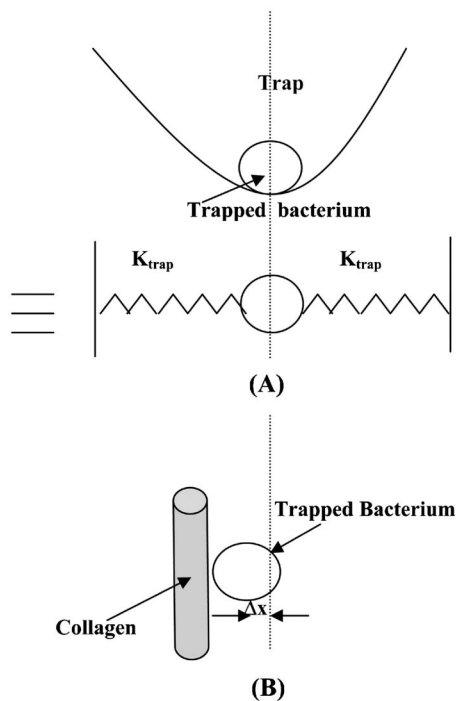


**Fig. 7** Drawing depicting measurement of interaction force of trapped *E. faecalis* bacterium with collagen substrate: (A) Stiffness of trap for *E. faecalis* bacterium in absence of collagen is determined using equipartition theorem method and (B) displacement  $\Delta x$  of the bacterium from its mean position (dotted line) in presence of collagen is a measure of the interaction force.

Calcium hydroxide has a high pH. Its high pH is normally used to kill bacteria in the root canal and is used in-between visits during RCT as an intracanal medicament. There may have been remaining effects of calcium hydroxide which were not fully removed by vortexing the membranes. The collagen membranes treated by calcium hydroxide may have altered the pH of collagen sufficiently to alter adhesion of *E. faecalis*. It is known that a slightly alkaline pH encourages *E. faecalis* adhesion.<sup>26</sup> An increase in the number of bacteria adhering to the membranes could also arise because of the presence of the divalent calcium ions. Previous studies have shown that calcium ions can aid in the formation of metallic ion bridges between oral bacteria.<sup>27</sup> Statistical analysis by one-way ANOVA, using multiple comparisons with  $p=0.05$ , showed that there was significant difference between the calcium hydroxide-treated group and all other groups. It is interesting to note that although sodium hypochlorite denatures collagen, the adherence of *E. faecalis* to it was much less than calcium hydroxide-treated collagen. Why this is so is not clear to us, but it seems that denaturation was not the only reason for an increase in bacteria adhering to the treated substrate.

**Table 3** Effect of treatment of collagen membranes with calcium on interaction force. Mean and standard deviation was calculated from four measurements.

Condition	Mean displacement of Bacteria ( $\mu\text{m}$ )	Power (mW)	Force (pN)
After 5 min near collagen (No Ca)	0.26	22	0.03 $\pm$ 0.02
Rupture of bond after 5 min near collagen (No Ca)	Away from collagen	36	0.38 $\pm$ 0.11
After 1 min near collagen (50% Ca)	0.25	22	0.04 $\pm$ 0.01
After 5 min near collagen (50% Ca)	0.43	22	0.9 $\pm$ 0.17
Rupture of bond after 5 min near collagen (50% Ca)	Away from collagen	180	2.1 $\pm$ 1.05

Although the definite sequence of irrigation during RCT is not yet established, clinicians may use demineralizing or chelating agents as the final irrigant to remove the smear layer. In so doing, collagenous surfaces are likely left exposed. If any *E. faecalis* is left alive in the root canal after treatment, then subsequent placement of calcium hydroxide may improve their chances of survival by biofilm formation because our results have indicated that the force of adhesion in the presence of calcium hydroxide is increased, and adhesion is the first step to biofilm formation.

The chlorhexidine-treated group had the least bacteria adhering. Chlorhexidine [chemical name: 2-[amino-[6-[amino-[amino-(4-chlorophenyl)amino-methylidene]amino-ethylidene]amino-hexylimino]methyl]-1-(4-chlorophenyl)guanidine; 2,3,4,5,6-pentahydroxyhexanoic acid] is a commonly used antibacterial compound used in health care for cleaning wounds<sup>28</sup> and in dentistry, in various forms, for controlling periodontitis.<sup>29</sup> The chlorhexidine molecule is a symmetrical di-cationic molecule, which has two charged centers that are at a relatively large distance apart. In an aqueous environment, the compound forms small aggregates (four monomers)<sup>30</sup> and had been shown to remain adsorbed on tooth surfaces.<sup>31</sup> In combination with calcium hydroxide, it was found to reduce the intracanal microbiota significantly and subsequently of periapical biofilm formation.<sup>32</sup> Chlorhexidine is known to have substantivity—the persistence of a residual activity on a surface for a period of time after application. Chlorhexidine, when used on oral tissues, including in root-canal dentine, has been reported to have substantivity for up to 12 weeks.<sup>33</sup> In our experiment, substantivity is likely to have contributed to why much fewer bacteria were adhering on the membranes soaked in chlorhexidine. Chlorhexidine substantivity clearly resides on the collagen despite our having vortexed the membranes at 450 G. Reduction of *E. faecalis* adherence would contribute to lower propensity for subsequent bacterial biofilm growth as well as eventual invasion and spread of infection.

Optical tweezers-based experiments highlighted that calcium hydroxide treatment increases adherence and adhesion forces of *E. faecalis* to type-I collagen. However, more studies are required to understand why there seems to be a maximum increase in the adhesive attraction between *E. faecalis* and type-I collagen in the presence of 50% saturated calcium hy-

droxide solution. The effects of differing root-canal disinfection regimes should also be investigated in the future.

## 5 Conclusions

Within the limitations of these experiments, we conclude that chlorhexidine is effective in preventing adhesion of *E. faecalis* ATCC 29212 to a type-I collagen membrane obtained from eggshells. The CLSM-based adherence assay showed that the treatment of the collagen type-I membrane with calcium hydroxide increased the adhesion of *E. faecalis*. The optical tweezers-based measurements show that presence of calcium hydroxide increased the force of attraction between the microorganism and type-I collagen.

## Acknowledgments

The authors thank Dr. Mrinalini Sharma, BMAID, RRCAT, Indore, for her support in bacteria culture during optical tweezers experiments. The funding from NSU-ARF FY05 Grant No. R-224-000-029-112 is gratefully acknowledged.

## References

- Hubert E. Schroeder, *Oral Structural Biology: Embryology, Structure, and Function of Normal Hard and Soft Tissues of the Oral Cavity and Temporomandibular Joints*, pp. 85–124, Georg Thieme, Stuttgart (1991).
- G. W. Marshall, Jr., S. J. Marshall, J. H. Kinney, and M. Balooch, "The dentin substrate: structure and properties related to bonding," *J. Dent.* **25**(6), 441–458 (1997).
- S. Karjalainen and E. Soderling, "Dentino-pulpal collagen and the incorporation of 3H-proline by sound and carious human teeth in vitro," *J. Biol. Buccale* **12**(4), 309–316 (1984).
- P. N. Nair, S. Henry, V. Cano, and J. Vera, "Microbial status of apical root canal system of human mandibular first molars with primary apical periodontitis after "one-visit" endodontic treatment," *Oral Surg. Oral Med. Oral Pathol. Oral Radiol. Endod.* **99**(2), 231–252 (2005).
- A. Kishen, S. George, and R. Kumar, "Enterococcus faecalis-mediated biomineralized biofilm formation on root canal dentine in vitro," *J. Biomed. Mater. Res. A* **77**(2), 406–415 (2006).
- R. M. Love, "Enterococcus faecalis—a mechanism for its role in endodontic failure," *Int. Endod. J.* **34**(5), 399–405 (2001).
- G. Sundqvist, D. Figdor, S. Persson, and U. Sjogren, "Microbiologic analysis of teeth with failed endodontic treatment and the outcome of conservative re-treatment," *Oral Surg. Oral Med. Oral Pathol. Oral Radiol. Endod.* **85**(1), 86–93 (1998).
- E. T. Pinheiro, B. P. Gomes, C. C. Ferraz, E. L. Sousa, F. B. Teixeira, and F. J. Souza-Filho, "Microorganisms from canals of root-filled



- teeth with periapical lesions," *Int. Endod. J.* **36**(1), 1–11 (2003).
9. J. F. Siqueira, Jr. and I. N. Rocas, "Polymerase chain reaction-based analysis of microorganisms associated with failed endodontic treatment," *Oral Surg. Oral Med. Oral Pathol. Oral Radiol. Endod.* **97**(1), 85–94 (2004).
  10. J. Ubbink and P. Schar-Zamaretti, "Probing bacterial interactions: integrated approaches combining atomic force microscopy, electron microscopy and biophysical techniques," *Micron* **36**(4), 293–320 (2005).
  11. F. Gaboriaud and Y. F. Dufrene, "Atomic force microscopy of microbial cells: application to nanomechanical properties, surface forces and molecular recognition forces," *Colloids Surf., B* **54**(1), 10–19 (2007).
  12. A. Razatos, Y. L. Ong, M. M. Sharma, and G. Georgiou, "Molecular determinants of bacterial adhesion monitored by atomic force microscopy," *Proc. Natl. Acad. Sci. U.S.A.* **95**(19), 11059–11064 (1998).
  13. V. Vadillo-Rodríguez, H. J. Busscher, W. Norde, J. de Vries, R. J. Dijkstra, I. Stokroos, and H. C. van der Mei, "Comparison of atomic force microscopy interaction forces between bacteria and silicon nitride substrata for three commonly used immobilization methods," *Appl. Environ. Microbiol.* **70**(9), 5441–5446 (2004).
  14. J. H. Hoh and C. A. Schoenenberger, "Surface morphology and mechanical properties of MDCK monolayers by atomic force microscopy," *J. Cell. Sci.* **107**(Pt 5), 1105–1114 (1994).
  15. Karl Otto Greulich, "Laser microbeam studies on unicellular organisms, cells and subcellular structures," in *Micromanipulation by Light in Biology and Medicine: The Laser Microbeam and Optical Tweezers*, 1st ed., p. 112, Birkhäuser, Boston (1999).
  16. D. A. Carrino, J. E. Dennis, T. M. Wu, J. L. Arias, M. S. Fernandez, J. P. Rodriguez, D. J. Fink, A. H. Heuer, and A. I. Caplan, "The avian eggshell extracellular matrix as a model for biomineralization," *Connect. Tissue Res.* **35**(1–4), 325–329 (1996).
  17. A. Ashkin, "Forces of a single-beam gradient laser trap on a dielectric sphere in the ray optics regime," in *Laser Tweezers in Cell Biology*, edited by Michael P. Sheetz, *Methods in Cell Biology* Vol. 55, pp. 1–27, Academic, San Diego (1998).
  18. S. L. Erlandsen, C. J. Kristich, and G. M. Dunny, "Ultrastructure of *Enterococcus faecalis* biofilms," *Biofilms* **1**, 131–137 (2004).
  19. R. E. Beltz, M. Torabinejad, and M. Poursmail, "Quantitative analysis of the solubilizing action of MTAD, sodium hypochlorite, and EDTA on bovine pulp and dentin," *J. Endod.* **29**(5), 334–337 (May 2003).
  20. T. Zurbruggen, C. E. del Rio, and J. M. Brady, "Post debridement retention of endodontic reagents: a quantitative measurement with radioactive isotope," *J. Endod.* **1**(9), 298–299 (1975).
  21. P. L. Mäkinen, D. B. Clewell, F. An, and K. K. Mäkinen, "Purification and substrate specificity of a strongly hydrophobic extracellular metalloendopeptidase ("gelatinase") from *Streptococcus faecalis* (strain OG1-10)," *J. Biol. Chem.* **264**(6), 3325–3334 (1989).
  22. B. R. Oguntebi, "Dentine tubule infection and endodontic therapy implications," *Int. Endod. J.* **27**(4), 218–222 (1994).
  23. J. L. Arias, O. Nakamura, M. S. Fernandez, J. J. Wu, P. Knigge, D. R. Eyre, and A. I. Caplan, "Role of type X collagen on experimental mineralization of eggshell membranes," *Connect. Tissue Res.* **36**(1), 21–33 (1997).
  24. R. M. Donlan, "Biofilms: microbial life on surfaces," *Emerg. Infect. Dis.* **8**(9), 881–890 (Sep 2002).
  25. S. George, A. Kishen, and K. P. Song, "The role of environmental changes on monospecies biofilm formation on root canal wall by *Enterococcus faecalis*," *J. Endod.* **31**(12), 867–872 (Dec 2005).
  26. G. Kayaoglu, H. Erten, and D. Orstavik, "Growth at high pH increases *Enterococcus faecalis* adhesion to collagen," *Int. Endod. J.* **38**(6), 389–396 (2005).
  27. R. K. Rose, "The role of calcium in oral streptococcal aggregation and the implications for biofilm formation and retention," *Biochim. Biophys. Acta* **1475**(1), 76–82 (2000).
  28. C. Y. Cho and J. S. Lo, "Dressing the part," *Dermatol. Clin.* **16**(1), 25–47 (1998).
  29. J. Cosyn and I. Wyn, "A systematic review on the effects of the chlorhexidine chip when used as an adjunct to scaling and root planing in the treatment of chronic periodontitis," *J. Periodontol.* **77**(2), 257–264 (2006).
  30. F. Sarmiento, J. M. del Rio, G. Prieto, D. Attwood, M. N. Jones, and V. Mosquera, "Thermodynamics of micelle formation of chlorhexidine digluconate," *J. Phys. Chem.* **99**, 17628–17631 (1995).
  31. R. N. Sodhi, H. A. Grad, and D. C. Smith, "Examination by X-ray photoelectron spectroscopy of the adsorption of chlorhexidine on hydroxyapatite," *J. Dent. Res.* **71**(8), 1493–1497 (1992).
  32. J. A. Soares, M. R. Leonardo, L. A. da Silva, M. Tanomaru Filho, and I. Y. Ito, "Effect of rotary instrumentation and of the association of calcium hydroxide and chlorhexidine on the antiseptics of the root canal system in dogs," *Pesqui. Odontol. Bras.* **20**(2), 120–126 (2006).
  33. S. Rosenthal, L. Spangberg, and K. Safavi, "Chlorhexidine substantivity in root canal dentin," *Oral Surg. Oral Med. Oral Pathol. Oral Radiol. Endod.* **98**(4), 488–492 (2004).